Stabilization of DC–DC buck converter with unknown constant power load via passivity-based control plus proportion-integration

He, Wei; Namazi, Mohammad Masoud; Koofigar, Hamid Reza; Amirian, Mohammad Ali; Blaabjerg, Frede

Published in:
IET Power Electronics

DOI (link to publication from Publisher):
10.1049/pel2.12205

Publication date:
2021

Document Version
Publisher's PDF, also known as Version of record

Received: 7 December 2020 | Revised: 11 July 2021 | Accepted: 26 September 2021

IET Power Electronics

DOI: 10.1049/pel2.12205

The Institution of Engineering and Technology WILEY

ORIGINAL RESEARCH PAPER

Stabilization of DC–DC buck converter with unknown constant power load via passivity-based control plus proportion-integration

Wei He[1] | Mohammad Masoud Namazi[2] | Hamid Reza Koofigar[2] | Mohammad Ali Amirian[3] | Frede Blaabjerg[4]

[1] School of Automation, Nanjing University of Information Science and Technology (NUIST), Nanjing, China

[2] Department of Electrical Engineering, University of Isfahan, Isfahan, Iran

[3] Department of Electrical and Computer Engineering, Isfahan University of Technology, Isfahan, Iran

[4] Energy Department, Aalborg University, Aalborg, Denmark

Correspondence
Wei He, School of Automation, Nanjing University of Information Science and Technology (NUIST), Nanjing 210044, China.
Email: hwei@nuist.edu.cn

Funding information
National Natural Science Foundation (NNSF) of China, Grant/Award Number: 61903196; Natural Science Foundation of Jiangsu Province of China, Grant/Award Number: BK20190773; Natural Science Foundation of the Jiangsu Higher Education Institutions of China, Grant/Award Number: 19KJB510042; Startup Foundation for Introducing Talent, Grant/Award Number: 2018r084

Abstract

It is known that constant power load (CPL) may cause a negative impedance, which seriously affects the stability of power system. In this paper, a new control algorithm for DC–DC buck converter feeding unknown CPL is proposed. First, under the assumption of known extracted power load, the standard passivity–based control (PBC) is presented to reshape the system energy and compensate for the negative impedance and a proportion-integration (PI) action around passive output is added to improve disturbance rejection performance, which forms the PBC plus PI (PBC+PI). Then, a parameter estimation algorithm is developed, based on immersion and invariance (I&I) technique, in order to online estimate the extracted power load. In the next step, the online estimation scheme is adopted to construct an adaptive strategy. Finally, the stability analysis of the cascaded system containing a closed-loop control system and observer error dynamics is conducted. Simulation and experimental results are demonstrated to validate the performance of the proposed controller.

1 | INTRODUCTION

Microgrid refers to a small-scale power system, which provides the power by utilizing controllable distributed power supplies (DPSs) in a certain area [1, 2]. Its proposal is to achieve flexibility and efficient application of DPSs and solve their grid-connection problem. The development and extension of microgrid can fully promote the large-scale access to DPS and renewable energy and provide highly reliable power for various forms of loads.

DC–DC converters are regarded as an essential device in microgrids, whose major role is to interface the renewable sources including solar, wind energy and fuel cell with load systems for realizing power transfer [3, 4]. A typical structure of the microgrid with generations and loads is displayed in Figure 1, where the load system is made up of converters connected in cascade and parallel forms, rectifier, LC filter circuit, motor drives, and resistive load. This case is also mentioned in [5]. It is noted that for a feeder system, the load system should be exactly modeled as constant power load (CPL) system [6]. The negative impedance caused by CPL will obviously decrease stability margin or even destabilize the power systems [7]. As a consequence, various control methods have been proposed to compensate for it and then make the equivalent damping positive. Meanwhile, the controller of voltage regulation is developed by employing large/small signal analysis methods.

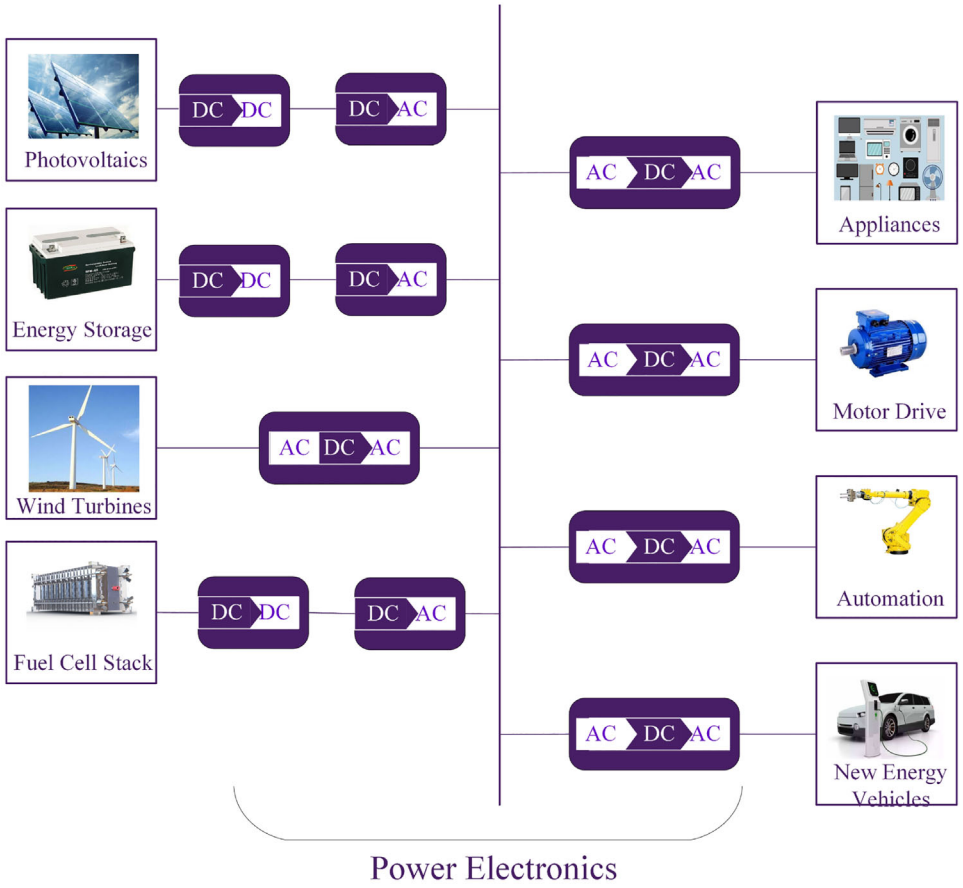

FIGURE 1 A typical structure of microgrid with generations and loads

An active damping approach is used to stabilize three traditional converters with CPLs including buck, boost and buck–boost [8]. Passive damping technique is employed for the voltage regulation of LC output filter with CPL [9]. It is reported in [10, 11] that sliding mode control is developed for buck converter and boost converter with CPLs. A controller based on local linearization technique is presented to control DC microgrids with CPL [12]. For DC power systems feeding CPL, a power shaping control scheme is devised [13, 14]. A H_∞ controller is developed to control buck converter with CPL [15]. However, the local linearization method based on the small-signal analysis is used. A composite controller integrating backstepping method with a disturbance observer is presented to deal with the voltage regulation problem of converters with CPL [16, 17]. Besides, to handle optimization problem of buck converters with CPL, model predictive control is introduced [18]. The papers [19–21] address the control problem of DC–DC converters with CPL under discontinous conduction mode (DCM). It is noted that the open-loop control systems of DC–DC converters feeding CPL under DCM are stable. This is a key result, which is different from the case of continous conduction mode (CCM). It is known that the existence of negative impedance caused by CPL will render the open-loop control system of converter under CCM unstable. It is observed from their analysis and simulation results that the closed-loop system under the controller proposed in [19–21] is unstable under CCM. Therefore, there is still a long way for researching the control problem of DC–DC converter with CPL under DCM from the theoretical view. The readers can refer to the reviews in [5, 22, 23] on this topic, which state the sphere of application of the aforementioned methods in some details.

Passivity-based control (PBC) based on the energy principle is one of the advanced nonlinear control methods [24, 25]. It is not surprising that there are a lot of results working on the PBC for DC–DC converters. To stress the key point, the representative works are reviewed here. For the simple case of the classical resistance load, in [24, 26, 27], the PBC is designed for DC–DC converters using Lagrangian approach. Borrowing these results, this control method is also proposed for ZVS quasi-resonant boost converter [28]. In [29, 30], the authors propose the PBC algorithm for boost converter under mixed conduction mode. It is noted that both controllers need the exact information of resistance load and input voltage, which can not be achieved in practical application. Further, in [31], the authors design an incremental passivity-based controller for boost converter with multiple disturbances. It is noted that the the use of generalized proportional integral observer can eliminate the affect of the time-varying disturbances on the system. In [32], the authors present a nonlinear controller for

switched reluctance-based wind system on the basis of the passivity theory. It is also adopted to address the voltage regulation problem of DC microgrids with ZIP loads [33]. Based on the port-controlled Hamiltonian structure, it is reported in [34, 35] that the authors propose a PI-PBC to stabilize a large class of power converters with the globally asymptotically stability. Following this work, the PI-PBC is used for controlling the dynamic wireless charging system, MMC multi-terminal HVDC systems and wind energy conversion system [36–38]. For the photovoltaic/battery hybrid power source system, an adaptive PBC is designed [39].

For the complicated case of constant power load, an adaptive energy shaping control is developed to control DC–DC buck–boost converter [40–42]. In [43–46], an interconnection and damping assignment PBC (IDA-PBC) is developed for DC–DC converters with CPL. The first problem of these works lies in that another sensor should be added to measure the output current for avoiding the measurement of CPL. Although this slightly simplifies the control design, the cost of the overall system will be inevitably increased. Second, the parameter perturbations will obviously affect their steady-state performance. Besides, an adaptive PBC is presented to stabilize boost converter with CPL and constant voltage load (CVL) [47]. However, for this work, it should be clearly noted that the basic requirement of PBC is not strictly satisfied since the zero dynamics with respect to inductor current is not attractive. Moreover, the PBC is applied to provide some guide-lines of the controller design for buck converter with constant power load [48–50]. Unfortunately, the unreasonable approximation results in that the PBC law is simplified as a traditional linear PID. Moreover, the integral action around tracking error may destabilize the system since it is lack of the complete stability analysis. It is noted that, when the system is affected by the large disturbance and variant operation condition, the poor performance will be obtained. The description on this problem can be found in [[23], Remark 4].

Being aware of the previous problem, the major purpose of this paper is to design an effective PBC+PI, which is of practical interest for the users. Besides, adopting immersion and invariance (I&I) method [51], a parameter observer is devised to estimate extracted power load. The contributions are presented.

(1) *A correct PBC is designed to stabilize DC–DC buck converter with CPL under large signal analysis.*
(2) *An outer-loop PI around passive output is added to enhance the transient and disturbance attenuation performance.*
(3) *An adaptive control strategy combining PBC+PI with I&I observer is validated by simulation and experiment studies.*

The remaining part of the paper is organized as follows: the model of DC–DC buck converter feeding CPL and control objectives are shown in Section 2. Based on the passivity theory and I&I technique, an adaptive controller is designed in Section 3. Sections 4 and 5 show the simulation and experimental results, respectively. The conclusion is given in Section 6.

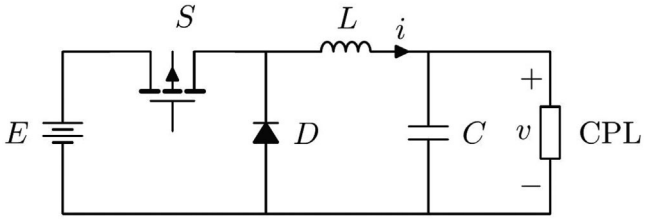

FIGURE 2 The circuit topology of DC–DC buck converter with a CPL

2 | MODEL DESCRIPTION AND PROBLEM FORMULATION

2.1 | Model of DC–DC buck converter with CPL

Figure 2 presents the circuit topology of a DC–DC buck converter with CPL. Considering continuous conduction mode (CCM) and using the average method, the model is given by

$$\begin{cases} L\dot{i} = -v + uE, \\ C\dot{v} = i - \dfrac{P}{v}, \end{cases} \tag{1}$$

where $i \in \mathbb{R}_{>0}$ denotes inductor current, $v \in \mathbb{R}_{>0}$ represents output voltage, $P \in \mathbb{R}_{>0}$ is CPL, $E \in \mathbb{R}_{>0}$ is input voltage, and $u \in [0, 1]$ is control input. It is straight forward to derive the equilibrium set of system (1)

$$\mathcal{E} := \{(i, v) \in \mathbb{R}^2_{>0} | i - \frac{P}{v} = 0\}.$$

2.2 | Control problem formation

The extracted power load P in (1) is assumed to be unknown, the control objectives are presented.

C1 Design a controller to regulate the output voltage v around desired value $v^\star$.
C2 Propose a parameter observer to achieve an adaptive control scheme.

For convenience, defining $x_1 := i, x_2 := v$, we obtain

$$\begin{cases} L\dot{x}_1 = -x_2 + Eu, \\ C\dot{x}_2 = x_1 - \dfrac{P}{x_2}. \end{cases} \tag{2}$$

The assignable equilibrium set is expressed as

$$\mathcal{E}_x := \left\{ x \in \mathbb{R}^2_{>0} \mid x_1 - \frac{P}{x_2} = 0 \right\}. \tag{3}$$

From (3), for given $x_{2\star}$, $x_{1\star}$ is calculated as follows

$$x_{1\star} = \frac{P}{x_{2\star}}.$$

3 | ADAPTIVE PBC+PI DESIGN

In this section, an adaptive PBC+PI is proposed to achieve the control objectives described in Section 2.2. The detailed design steps are given as follows.

- Under the assumption that the parameter P is known, a PBC+PI that asymptotically stabilizes a specified equilibrium $(x_{1\star},\ x_{2\star})$ is designed.
- A parameter observer is presented to estimate the unknown load P.
- By incorporating the parameter estimation algorithm into the controller, an adaptive control scheme is achieved.

To proceed with the following design, the system (2) is rewritten in Euler–Lagrange (EL) representation [24]

$$\mathcal{M}\dot{x} + \big(\mathcal{J} + \mathcal{R}(x)\big)x = Gu, \tag{4}$$

where $x = [x_1 \quad x_2]^T$, the generalized inertia $\mathcal{M} > 0$, damping matrix $\mathcal{R} \geq 0$, interconnection matrix $\mathcal{J} = -\mathcal{J}^T$ and G are expressed as

$$\mathcal{M} = \begin{bmatrix} L & 0 \\ 0 & C \end{bmatrix}, \mathcal{R} = \begin{bmatrix} 0 & 0 \\ 0 & \frac{P}{x_2^2} \end{bmatrix}, \mathcal{J} = \begin{bmatrix} 0 & 1 \\ -1 & 0 \end{bmatrix}, G = \begin{bmatrix} E \\ 0 \end{bmatrix}.$$

Differentiating the system energy function $H(x) = \frac{1}{2}x^T\mathcal{M}x$ gets the power balance equation

$$\dot{H} = \underbrace{ux_1E}_{\text{input power}} - \underbrace{\frac{P}{x_2}}_{\text{extracted power}},$$

which implies that the difference between input power and the extracted power is equal to the increase in the stored energy.

3.1 | PBC+PI design

3.1.1 | PBC

Here, based on the standard PBC methodology [24], a controller is proposed to stabilize the system (4).

Theorem 1. *Consider the system (4) with the control input*

$$u_{\text{PBC}} = \frac{1}{E}\left(L\left(\frac{-2Px_{2\star}}{Cx_2^3}\left(x_1 - \frac{P}{x_2}\right) + \dot{\omega}_2\right) + x_{2\star} + \omega_1\right), \tag{5}$$

where ω_1, ω_2 are the external input signals. Then, the closed-loop system is locally asymptotically stable.

Proof. First, we propose the reference dynamics of the system (4) as

$$\mathcal{M}\dot{x}_d + \big(\mathcal{J} + \mathcal{R}(x)\big)x_d = Gu - \omega, \tag{6}$$

where ω is defined as $\omega = [\omega_1 \quad \omega_2]^T$. Subtracting (6) from (4) and defining $e := x - x_d$, we derive the following error dynamics

$$\mathcal{M}\dot{e} + \big(\mathcal{J} + \mathcal{R}(x)\big)e = \omega. \tag{7}$$

Then, we reshape the function by assigning the desired energy function

$$V(e) = \frac{1}{2}e^\top\mathcal{M}e.$$

Differentiating the function V along the trajectory (7) with respect to time yields

$$\begin{aligned} \dot{V}(e) &= -e^\top(\mathcal{J} + \mathcal{R})e + e^\top\omega \\ &= -e^\top\mathcal{R}e + e^\top\omega \\ &< e^\top\omega, \end{aligned} \tag{8}$$

which clearly shows that the map $\omega \to e$ is passive with respect to V. On the other hand, the reference system (6) is equivalent to

$$\begin{cases} L\dot{x}_{1d} = -x_{2d} + Eu - \omega_1, \\ C\dot{x}_{2d} = x_{1d} - \dfrac{P}{x_2^2}x_{2d} - \omega_2. \end{cases} \tag{9}$$

Borrowing PBC methodology [24], $x_{2d} = x_{2\star}$ is fixed. Using second equation of (9), one obtains

$$x_{1d} = \frac{P}{x_2^2}x_{2\star} + \omega_2. \tag{10}$$

Differentiating x_{1d} in (10) and substituting it in the first equation of (9), the proposed PBC is given by

$$u_{\text{PBC}} = \frac{1}{E}\left(L\left(\frac{-2Px_{2\star}}{Cx_2^3}\left(x_1 - \frac{P}{x_2}\right) + \dot{\omega}_2\right) + x_{2\star} + \omega_1\right). \tag{11}$$

Now, from (8), the external signal ω can be designed as

$$\omega = -k_p e, \tag{12}$$

where the diagonal matrix $k_p \in \mathbb{R}^{2\times2} > 0$ is the control gain, $e_1 = x_1 - x_{1d}, e_2 = x_2 - x_{2\star}$. It is concluded that, the damping injection ω ensures that the Lyapunov function V decreases so that the closed-loop system is locally asymptotically stable. □

Remark 1. For standard PBC method, the zero dynamics of the system with respect to the output should be asymptotically stable [24]. For our design, there is no zero dynamics since the relative degree is two with respect to the output $x_2 - x_{2\star}$. However, the zero dynamics of the system with respect to $x_1 - x_{1\star}$ is unstable, which is stated in Proposition 1 of [23].

Remark 2. It is reported in [25, 52] that for PBC methodology, to enhance the anti-disturbance performance, an integral action around the passive output can be added.

3.1.2 | PI

The damping injection term (12) and an integral action are combined to form a PI controller around passive output.

Theorem 2. *In the system (4), an outer-loop PI controller is designed as*

$$\begin{cases} \omega = -k_p e - k_i \chi, \\ \dot{\chi} = e, \end{cases} \tag{13}$$

where the diagonal matrices $k_p \in \mathbb{R}^{2\times2} > 0, k_i \in \mathbb{R}^{2\times2} > 0$ are the damping injection parameters. The closed-loop system, formed by applying (5) and (13), is locally asymptotically stable with the Lyapunov function

$$W(e, \chi) = V(e) + \frac{1}{2} k_i \chi^T \chi. \tag{14}$$

Proof. Defining $\xi = [e \quad \chi]^T$, the closed-loop system is expressed as

$$\begin{bmatrix} M & 0 \\ 0 & k_i \end{bmatrix} \dot{\xi} + \begin{bmatrix} \mathcal{J} + \mathcal{R} + k_p & k_i \\ -k_i & 0 \end{bmatrix} \xi = 0. \tag{15}$$

By choosing the Lyapunov function (14) and differentiating the function W along (15) with respect to time, one yields

$$\begin{aligned} \dot{W} &< e^{\top} \omega + k_i \dot{\chi} \chi \\ &= -k_p e^T e - k_i e^T \chi + k_i e^T \chi \\ &= -k_p e^T e < 0. \end{aligned}$$

Based on the LaSalle–Yoshizawa theorem [53], the closed-loop system (15) is locally asymptotically stable provided that $y = e$ is a detectable output, that is,

$$y(t) = 0 \Rightarrow \lim_{t\to\infty} (e(t), \chi(t)) = (0, 0).$$

From (15), fixing $y = e = 0$, we have $\chi = 0$. The proof is completed. □

Finally, the PBC+PI controller is proposed by integrating (5) with (13).

Remark 3. Although the control law (5) contains a differential term $\dot{\omega}_2$, it can be written as $\dot{\omega}_2 = -\frac{k_{p2}}{C}(x_1 - \frac{P}{x_2}) - k_{i_2}(x_2 - x_{2\star})$. Hence, there is no problem about noise amplification caused by differential action.

Remark 4. Compared with the traditional PBC methodology [24], adding the explicit differentiation of x_{1d} to obtain an explicit expression of the controller is an original contribution of this paper.

Remark 5. As explained in Section 3.1 of [24], the standard PBC performs a 'partial inversion' of the systems dynamics. Indeed, the controller is a copy of part of the systems equations with the remaining states set equal to constants-plus some damping injection terms that vanish at the equilibrium. These design rules are conducted in (6)–(11).

Remark 6. Compared with the existing results [48–50], this method has three main advantages.

- In [48–50], to obtain the explicit expression of the controller, x_{1d} is equal to $x_{1\star}$ on the basis of $x_{2d} = x_{2\star}$. However, x_{1d} has inherent behavior itself, which is shown in (10). $x_{1d} = x_{1\star}$ holds only under steady state.
- Although the controller design and stability analysis of [48–50] are based on a large signal model, the designed PBC is equivalent to a traditional PID controller. In the case, in [48–50], the designed PBC based on large signal analysis is no longer valid. As a result, the main contribution of our paper is to propose a correct PBC with strict stability analysis.
- As shown in [48–50], the integral action around the error $x_{2\star} - x_2$ may destabilize the system except the selection of very small k_i. This is due to the uncompleted stability analysis. The conservative selection of control gain will degrade the performance. Therefore, another contribution of this paper is to add a PI (13)—with all positive gains—around passive output, which will effectively improve the transient and anti-disturbance performance. Importantly, the strict stability analysis is given in Theorem 2.

3.2 | Parameter observer design

Here, based on the I&I technique [51], an observer can be developed to reconstruct P, which is now assumed to be unmeasured.

Theorem 3. *For the system (2), we design parameter observer*

$$\begin{cases} \hat{P} = q - \dfrac{1}{2}\gamma C x_2^2, \\ \dot{q} = \gamma x_1 x_2 - \gamma \hat{P}, \end{cases} \tag{16}$$

where the observer gain $\gamma > 0$. *Defining the estimate error* $\tilde{P} = P - \hat{P}$, *one has*

$$\lim_{t\to\infty} \tilde{P}(t) = 0. \tag{17}$$

Proof. Differentiating the estimate error $\tilde{P}$ along the trajectories (2) and (16), one gets

$$\begin{aligned} \dot{\tilde{P}} &= -\dot{\hat{P}} \\ &= \dot{q} - \gamma x_2 (x_1 - \frac{P}{x_2}) \\ &= -\gamma \tilde{P}, \end{aligned}$$

which gives the convergence property (17). □

3.3 | Adaptive control design

Substituting the estimate $\hat{P}$ of (16) in (5), (13), the adaptive control law is formed by

$$\begin{cases} \hat{u}_{\mathtt{PBC+PI}} = \dfrac{1}{E}\left(L\left(\dfrac{-2\hat{P}x_{2\star}}{C x_2^3}\left(x_1 - \dfrac{\hat{P}}{x_2} \right) + \dot{\hat{\omega}}_2 \right) + x_{2\star} + \hat{\omega}_1 \right), \\ \hat{\omega} = -k_p \hat{e} - k_i \hat{\chi}, \\ \dot{\hat{\chi}} = \hat{e}, \\ \hat{e} = \begin{bmatrix} x_1 - \hat{x}_{1d} \\ x_2 - x_{2\star} \end{bmatrix}, \\ \hat{x}_{1d} = \dfrac{\hat{P}}{x_2^2} x_{2\star} + \omega_2. \end{cases} \tag{18}$$

We write the adaptive controller (18) in the perturbed form

$$\begin{aligned} \hat{u}_{\mathtt{PBC}} &= u_{\mathtt{PBC+PI}} + \varphi_1(x)\tilde{P}, \\ \hat{\omega} &= \omega + \varphi_2(x)\tilde{P}, \end{aligned} \tag{19}$$

where $\varphi_1(x), \varphi_2(x)$ are the properly defined functions. Therefore, applying the form (19) in system (4) and considering the observer error dynamics, the extended system can be obtained

$$\begin{cases} \begin{bmatrix} M & 0 \\ 0 & k_i \end{bmatrix} \dot{\xi} + \begin{bmatrix} \mathcal{J} + \mathcal{R} + k_p & k_i \\ -k_i & 0 \end{bmatrix} \xi = \varphi(x)\tilde{P}, \\ \dot{\tilde{P}} = -\gamma \tilde{P}. \end{cases} \tag{20}$$

where $\varphi(x) := [\varphi_1, \varphi_2]^T$. From Theorems 1 and 2, it is noted that the system (20) is asymptotically stable when $\tilde{P} = 0$. Therefore, borrowing the asymptotic result of the cascaded system reported in Proposition 4.1 of [54], the locally asymptotic stability of the system (20) is established.

Remark 7. The papers [40–42] are focus on the control problem of DC–DC buck–boost converter with CPL. Moreover, the control performance of the works [40–42] is sensitive to the variations of the circuit parameters L, C, E since their exact knowledge is needed. In this paper, we successfully address the voltage regulation problem of DC–DC buck converter via an adaptive PI-PBC. Importantly, an integration around the passive output is added to further improve the robustness against the parameter perturbations.

TABLE 1 Simulation/experimental set-points and physical parameters

Parameter	Symbol (unit)	Value
Input voltage	E(V)	24
Reference output voltage	$x_{2\star}$(V)	12
Gain	$x_{2\star}/E$	0.5
Nominal extracted power	P(W)	14
Inductance	$L(\mu$H)	110
Capacitance	$C(\mu$F)	630

4 | SIMULATION RESULTS

A simulation study, which verifies the effectiveness of the proposed adaptive PBC+PI (18), is carried out via 2019bMatlab/Simulink. The control structure of DC–DC buck converter with CPL is shown in Figure 3, where a buck converter with resistance is regarded as a CPL. The circuit parameters are shown in Table 1. To clearly state the results, the following simulation cases are considered.

4.1 | Tracking performance

To clearly investigate the tracking performance of the adaptive control scheme, the cases of different references and initial conditions are taken into account. The simulations are demonstrated with initial conditions as

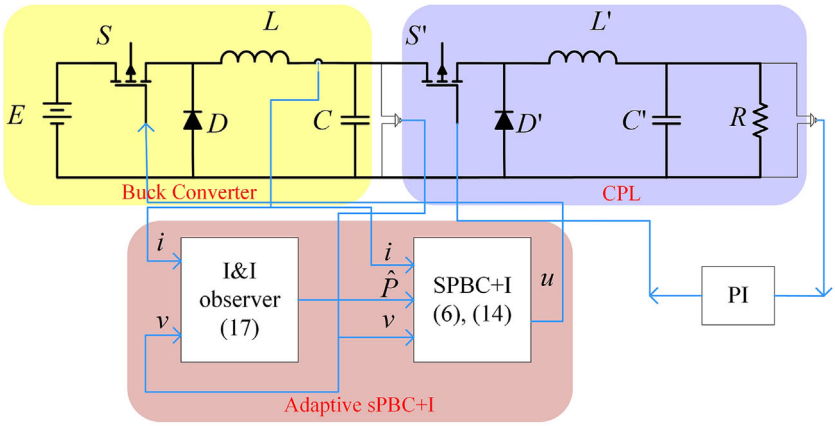

FIGURE 3 The control structure of DC–DC buck converter with a CPL

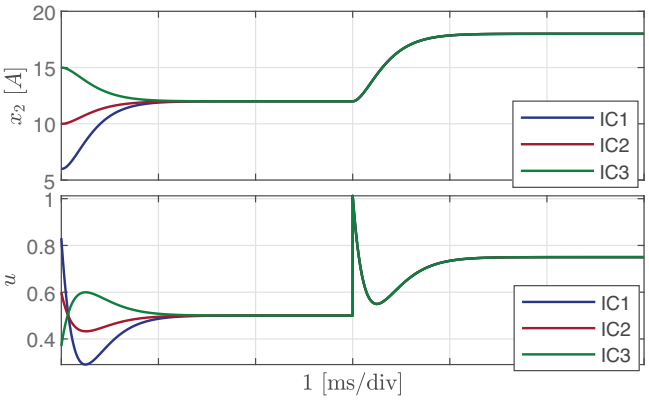

FIGURE 4 Variable response curves of DC–DC buck converter with CPL under proposed adaptive PBC+PI with $k_{p_1} = k_{p_2} = 1, k_{i_1} = k_{i_2} = 0.5$, in the presence of different initial conditions and reference $x_{2\star}$ from 12 V to 18 V

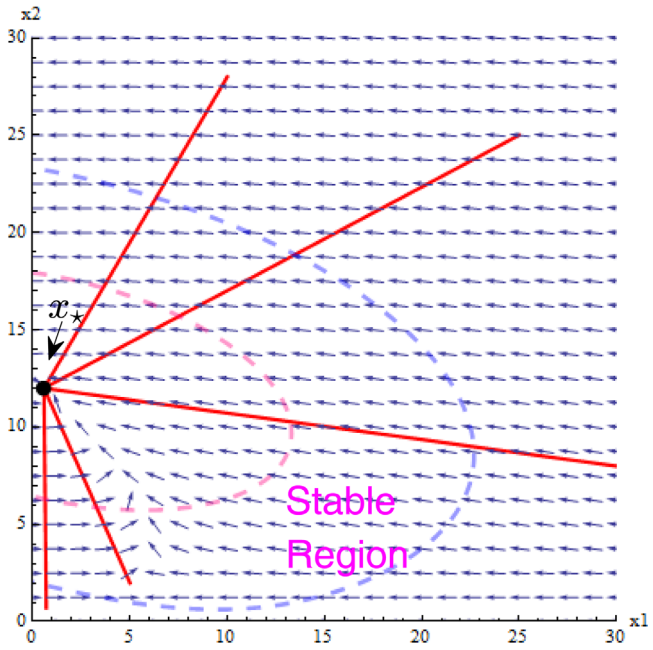

FIGURE 5 Phase portrait of closed-loop system under the proposed controller with $k_{p_1} = k_{p_2} = 1, k_{i_1} = k_{i_2} = 1$

IC1. $x(0)^T = [0.1,\ 6]$,

IC2. $x(0)^T = [0.1,\ 10]$,

IC3. $x(0)^T = [0.1,\ 15]$.

Figure 4 reveals the response curves of the output voltage and control input of the buck converter with CPL under adaptive PBC+PI with different initial conditions and $x_{2\star}$ ranging from 12 V to 18 V. It is depicted in this figure that the output voltage is capable of converging to the desired value. In addition, as predicted by theory, when the considered initial condition is more away from equilibrium, the larger initial energy consumption is required. Besides, the phase portrait of closed-loop system is shown in Figure 5. It is assumed that the parameter P has been estimated exactly. The red lines denote the diverse state trajectories from different initial conditions. As revealed in figure, the state trajectories converge to $x_\star$. The stable region is shown by the dotted areas. It is noted that this domain is only estimated by choosing the initial condition. It is observed that the actual stable region is very large except the neighbour of zero.

4.2 | Gain sensitivity analysis

4.2.1 | Control gain

For assessing the control gain sensitivity and disturbance rejection performance, the step variation of the power load and input voltage is considered, respectively.

First, the parameter P ranges from 7 W to 14 W. The response curves of both states are illustrated in Figure 6. In the figure, it is seen that larger gains k_{p_1}, k_{p_2} give smaller recovery time. It is noted that the parameter observer and integral action simultaneously eliminate the influence of the variation of the power load P on the system, which brings a nice transient performance.

Subsequently, we consider that the input voltage E is changed from 24 V to 36 V. The integral action around passive output is able to suppress the influence of parameter pertur-

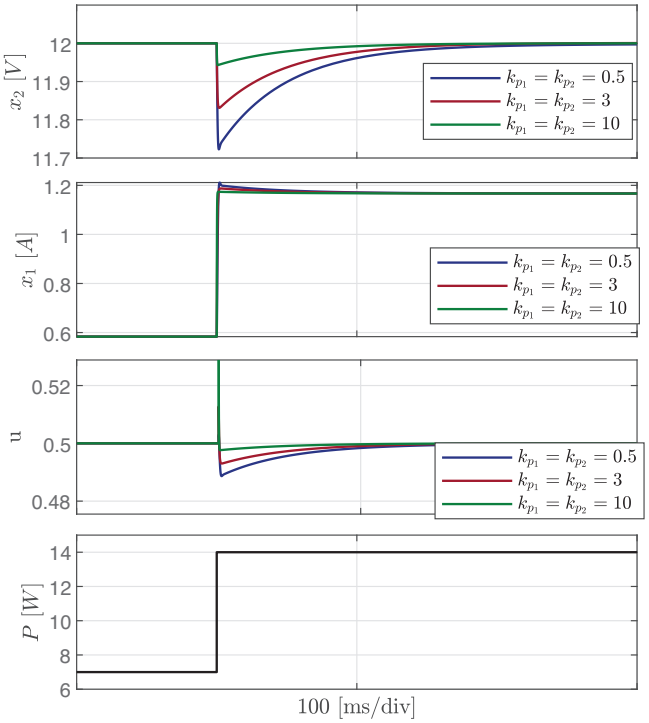

FIGURE 6 Variable response curves of DC–DC buck converter with CPL under proposed adaptive PBC+PI with different k_p and $k_{i_1} = k_{i_2} = 1$, in the presence of step change in P

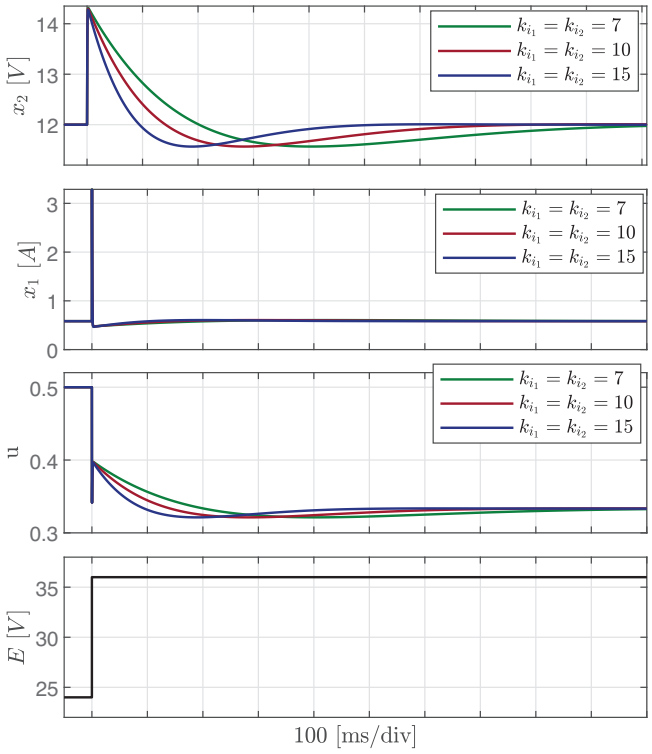

FIGURE 7 Variable response curves of DC–DC buck converter with CPL under proposed adaptive PBC+PI with different k_i and $k_{p_1} = k_{p_2} = 3$, in the presence of step change in E

bation on the system. Figure 7 shows the response curves of both states and control input under adaptive PBC+PI with different gains k_{i_1}, k_{i_2}. As seen in figure, the larger gains k_{i_1}, k_{i_2} have a better disturbance rejection performance. We estimate the system bandwidth by checking rise time. It is observed from Figure 4 that the rise time is about 1.5 ms. It is known that this time and the bandwidth are negatively correlated, that is,

$$BW = \frac{3.5}{t_r},$$

where BW and t_r denote the bandwidth and rise time, respectively. It is known that the better transient performance of closed-loop system needs larger bandwidth BW. It is observed from Figures 6 and 7 that the controller parameters will affect the rise time. However, the more nice noise-reducing performance requires smaller bandwidth BW. Hence, it needs to consider a trade-off between transient and noise-reducing performance for choosing the gains $k_{p_1}, k_{p_2}, k_{i_1}, k_{i_2}$.

4.2.2 | Observer gain

To evaluate the transient performance of the parameter observer, different observer gains γ are chosen with a fixed control gain $k_{p_1} = k_{p_2} = 1, k_{i_1} = k_{i_2} = 5$. As shown in Figure 8, a more quick convergence rate is achieved by a larger gain.

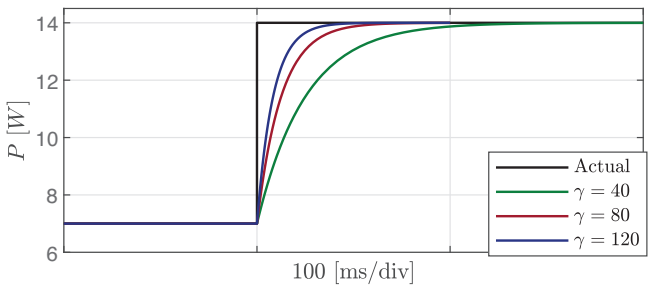

FIGURE 8 The transient of I&I load observer with different observer gains γ

4.3 | Adaptive PBC+PI versus classical PI

Now the comparison of the performances of the proposed control and a classical PI controller is conducted. To this end, the design and stability analysis of PI controller are first given.

For the system in (2), a PI controller around tracking error is designed as

$$u_{\mathrm{PI}} = \bar{k}_p \bar{e} + \bar{k}_i \int \bar{e}, \tag{21}$$

where $\bar{k}_p > 0, \bar{k}_i > 0$ are the control gains and $\bar{e} := x_2 - x_{2\star}$. Substituting (21) in system (2), one yields

$$\begin{cases} L\dot{x}_1 = -rx_1 - x_2 + (\bar{k}_p\bar{e} + \bar{k}_i\xi)E, \\ C\dot{x}_2 = x_1 - \dfrac{P}{x_2}, \\ \dot{\xi} = \bar{e}, \end{cases} \tag{22}$$

where ξ is an extended state and r is the parasitic resistance. Linearizing system (22) around the equilibrium, the system Jacobian matrix is obtained

$$J := \begin{bmatrix} -\dfrac{r}{L} & \dfrac{\bar{k}_pE - 1}{L} & \dfrac{\bar{k}_iE}{L} \\ \dfrac{1}{C} & \dfrac{P}{Cx_{2\star}^2} & 0 \\ 0 & 1 & 0 \end{bmatrix}. \tag{23}$$

To ensure the locally asymptotic stability of the system, the eigenvalues of matrix J defined in (23) should have negative real parts. To the end, the characteristic polynomial of (23) is given by

$$s^3 + a_1s^2 + a_2s + a_3 = 0, \tag{24}$$

where

$$\begin{aligned} a_1 &:= \frac{Crx_{2\star}^2 - LP}{CLx_{2\star}^2}, \\ a_2 &:= \frac{x_{2\star}^2 - Pr - E\bar{k}_px_{2\star}^2}{CLx_{2\star}^2}, \\ a_3 &:= \frac{-E\bar{k}_i}{CL}. \end{aligned}$$

Borrowing the Routh–Hurwitz criterion, the following conditions should be satisfied

$$a_1 > 0, a_2 > 0, a_3 > 0, a_1a_2 - a_3 > 0.$$

Equivalently, the stability condition may be given by

$$\begin{cases} \bar{k}_i < 0, \\ r > \dfrac{LP}{Cx_{2\star}^2}, \\ \bar{k}_p < \dfrac{\bar{k}_iCLx_{2\star}^2}{Crx_{2\star}^2 - LP} + \dfrac{x_{2\star}^2 - Pr}{Ex_{2\star}^2}. \end{cases} \tag{25}$$

From the condition in (25), the selection of control gains k_p, k_i depends on $E, P, x_{2\star}$. When the system is largely influenced by parameter perturbations and variant conditions, the performance of the system with classical PI under small signal analysis will be unsatisfactory.

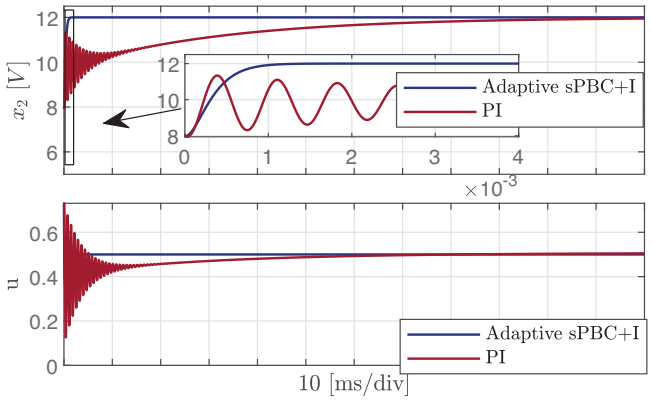

FIGURE 9 A comparison of output voltage x_2 and control input u between the proposed adaptive PBC+PI with $k_{p_1} = k_{p_2} = 1, k_{i_1} = k_{i_2} = 5$ and classical PI with $\bar{k}_p = -0.1, \bar{k}_i = -3$

Remark 8. It is observed that the parasitic resistance r is considered in the system (22). It is concluded from the condition (25) that, when $r = 0$, the closed-loop system is unstable. Hence, this imposes an extra limit on the system parameter. However, in our design, there is no restriction on it.

A comparison of transient performances of the proposed controller and classic PI is shown in Figure 9. The rise time under the former is about 1 ms, whereas that of the latter is 120 ms. It is obviously observed that the proposed scheme possesses the nice transient performance. One intuitive idea to improve the transient performance of classical PI is to increase $\bar{k}_p, \bar{k}_i$. However, it needs larger initial energy consumption in comparison with designed control law. Even, this results in that the control input u of classical PI may be beyond the constraint $[0, 1]$, which can not be achieved in practical application.

5 | EXPERIMENTAL RESULTS

The experiment parameters are identical with those in simulation study given in Table 1. Figure 10 reveals the experimental setup. The feeder buck converter uses a MOSFET switch instead of the diode to increase efficiency, which is a synchronous buck converter. The input voltage level is also adjustable from 18 V to 36 V, and the output voltage ranges from 2 V to 25 V. The working frequency of the converter is 100 kHz. The main processor, which is responsible for achieving the control algorithm and generating the switching pulses, is STM32F0K6 with the arm processing core ARM-Coretex-M0. This processor can transmit data with other devices or computers to monitor and send commands through serial communication. Converter protections includes overcurrent, input overvoltage, input under voltage, and output or input short circuit.

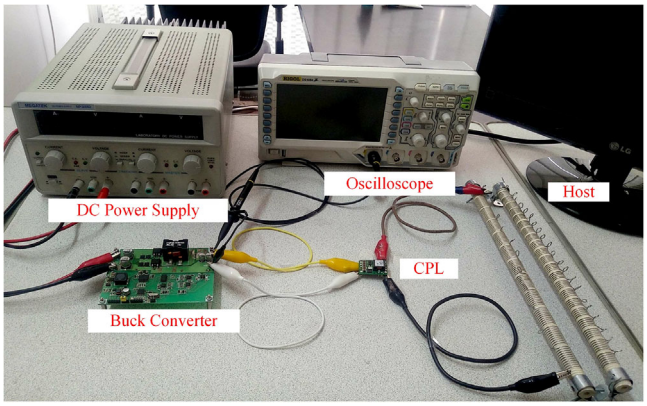

FIGURE 10 The experimental setup of DC–DC buck converter with CPL

The CPL is a non-isolated buck converter with resistance from TDK corporation model i6A4W product family, which is stabilized by a classical PI controller. It is capable of operating from a wide input voltage of up to 9 V to 53 V, and the output voltage can be adjustable from 3.3 V to 15 V.

To further illustrate the nice performance of proposed controller, the experimental comparison between adaptive PBC+PI and classical PI is carried out. The testing situations of simulation study are still considered in experiment. It is noted that the power of the experiment setup is low. Although it can not satisfy the requirement of the microgrids applications, in view of the reported theoretical analysis, it is certain that the proposed controller is also applicable to high power equipments-provided the assumed mathematical model remains valid and that components with similar efficiencies are used.

First, we consider that the reference $x_{2\star}$ is supposed to have two step changes, which ranges from 11 V to 16 V to 14 V. To show the nice tracking performance, a bigger change of the reference $x_{2\star}$ is also tested, which varies from 4 V to 20 V. The gains are chosen as $k_{p_1} = k_{p_2} = 1, k_{i_1} = k_{i_2} = 0.1, \gamma = 60$. Using the Ziegler–Nichols method, the optimal gains of the classical PI controller is chosen as $\bar{k}_p = -0.1, \bar{k}_i = -3$. The experimental waveforms of output voltage v, inductor current i and output current $i_{\mathtt{load}}$ of DC–DC buck converter with CPL under the proposed adaptive PBC+PI is presented in Figure 11. Figure 12 shows the result of classical PI controller. It is observed from the aforementioned figures that the transient performance under the former is better than that of the latter. Indeed, during the startup, the convergence time of closed-loop system under designed controller is about 0.2 s, whereas that of PI is approximate to 1.5 s. A trade-off among various performances including transient and robustness should considered when choosing classical PI gains. Nevertheless, due to the fact that the proposed controller is based on the large signal analysis and adaptive algorithm, the proper gains are selected so that a better performance can be obtained.

Subsequently, the robustness performance of both controllers in the presence of step change in P is tested when

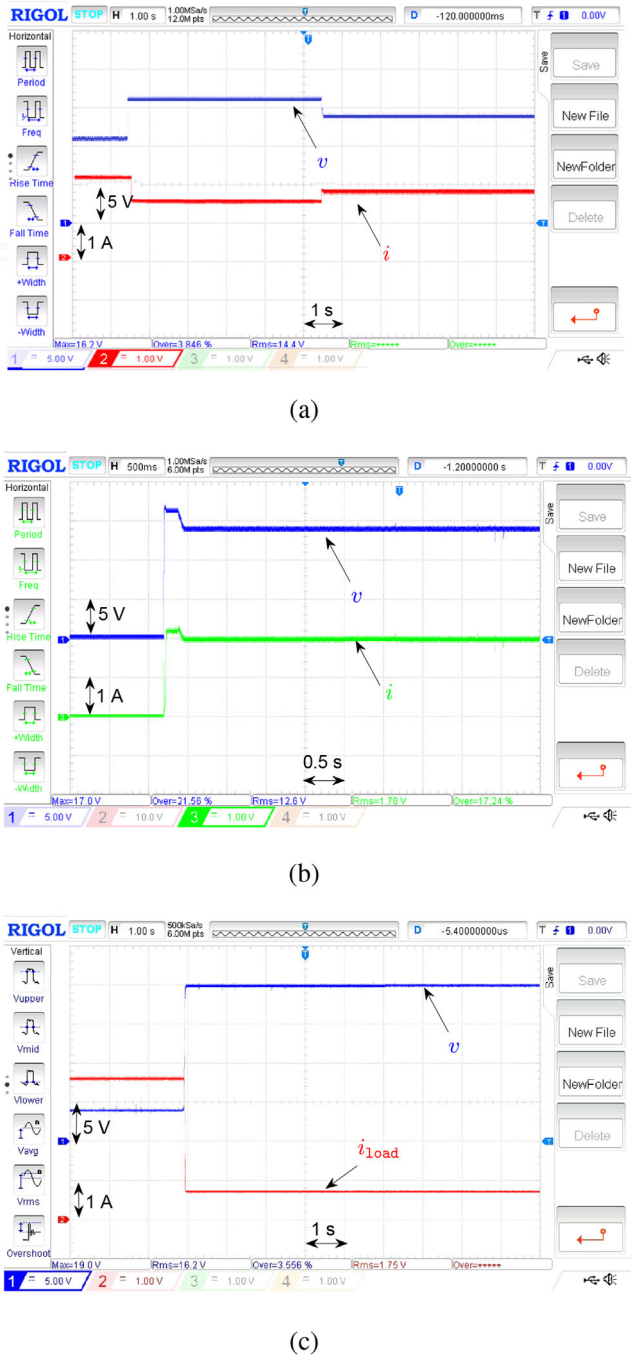

FIGURE 11 Response curves of output voltage v, inductor current i and output current $i_{\mathtt{load}}$ of DC–DC buck converter with CPL under adaptive PBC+PI. (a) $x_{2\star}$ ranges from 11 V to 16 V to 14 V. (b) Transient. (c) $x_{2\star}$ ranges from 4 V to 20 V

$x_{2\star} = 12$ V. It varies from 12 W to 24 W. In addition, a wider range of step change in P is considered to test the robustness of the designed controller, which changes from 7 W to 35 W. The experimental waveforms of output voltage, inductor current and output load $i_{\mathtt{load}}$ under adaptive PBC+PI and classical PI are shown in Figure 13. It is seen that the output voltage under designed control law offers an almost flat response with the step change in P, which illustrates the efficacy of

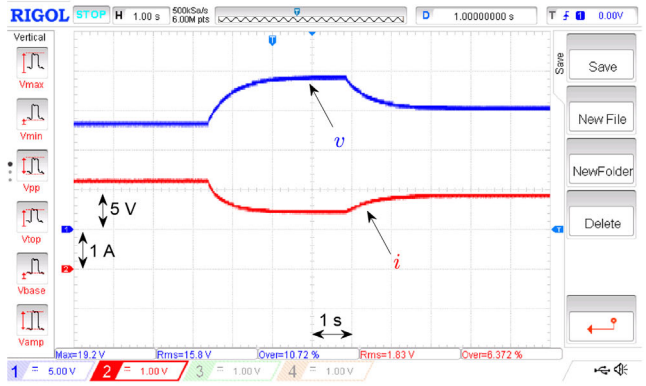

(a)

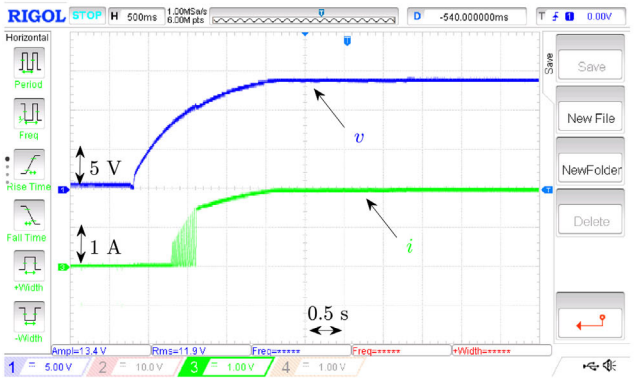

(b)

FIGURE 12 Response curves of output voltage v and inductor current i of DC–DC buck converter with CPL under classical PI. (a) Step change in $x_{2\star}$. (b) Transient

the adaptive capacity of the proposed controller. However, it is observed that the output voltage under classical PI has a longer recovery time. As a consequence, compared with the classical PI controller, the proposed method reveals the superiority in tracking and transient performances. Next, the experiment of the step change in E is carried out. In Figure 14, it is seen that although the input voltage E ranges from 18 V to 34 V, the output voltage still stays around 15 V. This demonstrates a nice robustness against the variation of input voltage.

Although it is supposed that this converter works in CCM, the system under the proposed controller shows a nice robustness against discontinuous conduction mode (DCM). It is noted that the adopted buck converter is a synchronous buck converter. To exactly show the result of DCM for traditional buck converter, the DCM for synchronous buck converter is done by adding control circuitry that detects the current through the MOSFET and turns it off when the current is zero in order to block any negative inductor current. Hence, the MOSFET effectively functions as a diode that enables the synchronous buck converter to operate in the DCM. It is seen in Figure 15 that the converter works in DCM. The waveform of output voltage contains a little big noise, but it still stays around the desired value.

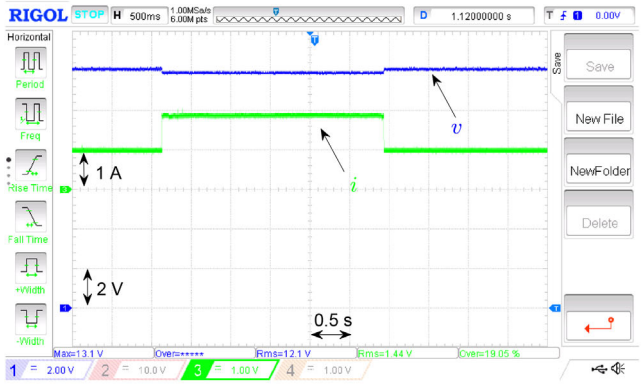

(a)

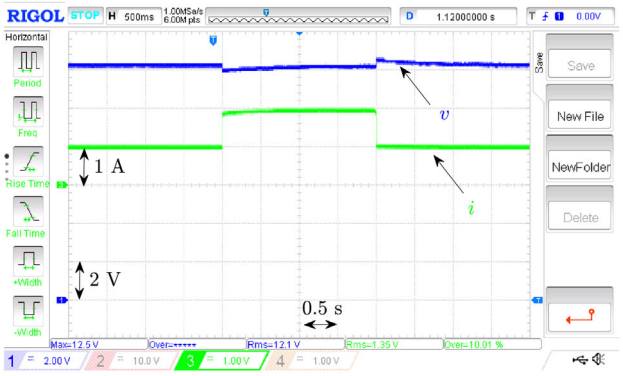

(b)

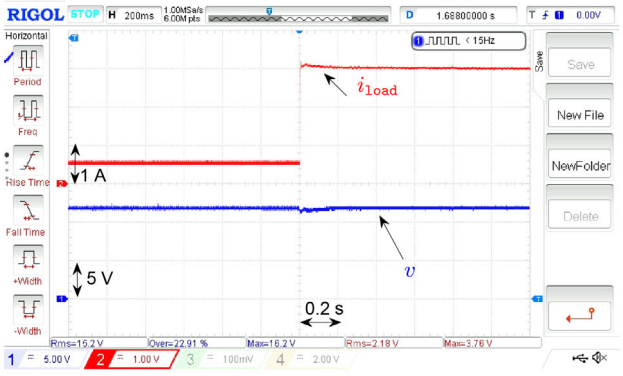

(c)

FIGURE 13 Response curves of output voltage v, inductor current i and output current i_{load} of DC–DC buck converter with CPL in the presence of step change in P. (a) Adaptive PBC+PI. $k_{p_1} = k_{p_2} = 1, k_{i_1} = k_{i_2} = 0.1$. P ranging from 12 W to 24 W. (b) Classical PI with $\bar{k}_p = -0.1, \bar{k}_i = -3$. P ranging from 12 W to 24 W. (c) Adaptive PBC+PI. $k_{p_1} = k_{p_2} = 1, k_{i_1} = k_{i_2} = 0.1$. P ranging from 7 W to 35 W

6 | CONCLUSION

The adaptive control problem for DC–DC buck converter with CPL was investigated in this paper. First, based on passivity, a PBC plus an outer-loop PI action was designed to stabilize DC–DC buck converter with CPL and then improve the transient and disturbance rejection performance. Subsequently, the parameter observer was proposed to estimate power load. Then, an adaptive controller

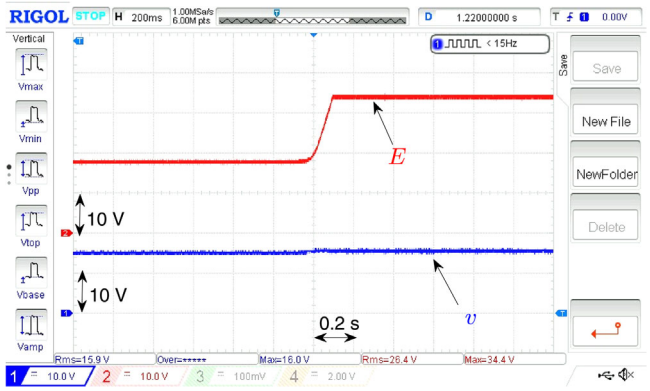

FIGURE 14 Response curve of DC–DC buck converter with CPL in the presence of step change in E from 18 V to 34 V. $P = 14$ W

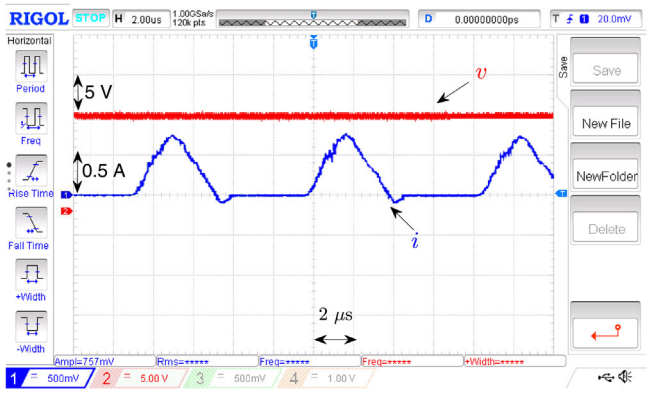

FIGURE 15 Response curves of DC–DC buck converter with CPL under DCM. $x_{2\star} = 12$ V

was developed by incorporating the estimated parameter into PBC+PI. Finally, the simulation and experimental results are given to assess the effectiveness of the proposed controller.

ACKNOWLEDGEMENTS

This research was supported in part by the National Natural Science Foundation (NNSF) of China (Grant No. 61903196), the Natural Science Foundation of Jiangsu Province of China (Grant No. BK20190773), the Natural Science Foundation of the Jiangsu Higher Education Institutions of China (Grant No. 19KJB510042), and the Startup Foundation for Introducing Talent of NUIST (Grant No. 2018r084).

DATA AVAILABILITY STATEMENT

The data that support the findings of this study are available from the corresponding author upon reasonable request.

CONFLICT OF INTEREST

The authors declare that there are no financial and personal relationships with other people or organizations that can inappropriately influence our work. We declare that there are no conflicts of interest to this work.

ORCID

Wei He https://orcid.org/0000-0001-7006-8885
Mohammad Masoud Namazi https://orcid.org/0000-0002-0270-0348

REFERENCES

1. Hossain, M., Rahim, N., et al.: Recent progress and development on power dc-dc converter topology, control, design and applications: A review. Renewable Sustainable Energy Rev. 81, 205–230 (2018)
2. Dragičević, T., Lu, X., Vasquez, J.C., Guerrero, J.M.: Dc microgridsâ‡part i: A review of control strategies and stabilization techniques. IEEE Trans. Power Electron. 31(7), 4876–4891(2015)
3. Singh, S., Fulwani, D., Kumar, V.: Robust sliding-mode control of dc/dc boost converter feeding a constant power load. IET Power Electron. 8(7), 1230–1237 (2015)
4. Yang, J., Cui, H., Li, S., Zolotas, A.: Optimized active disturbance rejection control for dc-dc buck converters with uncertainties using a reduced-order gpi observer. IEEE Trans. Circuits Syst. I: Regul. Pap. 65(2), 832–841 (2017)
5. Singh, S., Gautam, A.R., Fulwani, D.: Constant power loads and their effects in dc distributed power systems: A review. Renewable Sustainable Energy Rev. 72, 407–421 (2017)
6. Emadi, A., Khaligh, A., Rivetta, C.H., Williamson, G.A.: Constant power loads and negative impedance instability in automotive systems: definition, modeling, stability, and control of power electronic converters and motor drives. IEEE Trans. Veh. Technol. 55(4), 1112–1125 (2006)
7. Barabanov, N., Ortega, R., Griñó, R., Polyak, B.: On existence and stability of equilibria of linear time-invariant systems with constant power loads. IEEE Trans. Circuits Syst. I: Regul. Pap. 63(1), 114–121 (2015)
8. Rahimi, A.M., Emadi, A.: Active damping in dc/dc power electronic converters: A novel method to overcome the problems of constant power loads. IEEE Trans. Ind. Electron. 56(5), 1428–1439 (2009)
9. Cespedes, M., Xing, L., Sun, J.: Constant-power load system stabilization by passive damping. IEEE Trans. Power Electron. 26(7), 1832–1836 (2011)
10. Fulwani, D.K., Singh, S.: Mitigation of Negative Impedance Instabilities in DC Distribution Systems: A Sliding Mode Control Approach. Springer, Singapore (2016)
11. Zhao, Y., Qiao, W., Ha, D.: A sliding-mode duty-ratio controller for dc/dc buck converters with constant power loads. IEEE Trans. Ind. Appl. 50(2), 1448–1458 (2013)
12. Liu, Z., Su, M., Sun, Y., Han, H., Hou, X., Guerrero, J.M.: Stability analysis of dc microgrids with constant power load under distributed control methods. Automatica 90, 62–72 (2018)
13. Wang, J., Howe, D.: A power shaping stabilizing control strategy for dc power systems with constant power loads. IEEE Trans. Power Electron. 23(6), 2982–2989 (2008)
14. Mayo Maldonado, J., Ruiz Martinez, O., Escobar, G., Maupong, T., Valdez Resendiz, J., Rosas Caro, J.: Power shaping control of dc–dc converters with constant power loads. Control Eng. Pract. 105, 104639 (2020)
15. Boukerdja, M., Chouder, A., Hassaine, L., Bouamama, B.O., Issa, W., Louassaa, K.: h_∞ based control of a dc/dc buck converter feeding a constant power load in uncertain dc microgrid system. ISA Trans. 105, 278–295 (2020)
16. Lin, P., Zhang, C., Wang, P., Xiao, J.: A decentralized composite controller for unified voltage control with global system large-signal stability in dc microgrids. IEEE Trans. Smart Grid 10(5), 5075–5091 (2018)
17. Xu, Q., Zhang, C., Wen, C., Wang, P.: A novel composite nonlinear controller for stabilization of constant power load in dc microgrid. IEEE Trans. Smart Grid 10(1), 752–761 (2017)
18. Xu, Q., Yan, Y., Zhang, C., Dragicevic, T., Blaabjerg, F.: An offset-free composite model predictive control strategy for dc/dc buck converter feeding constant power loads. IEEE Trans. Power Electron. 35(5), 5331–5342 (2019)
19. Rahimi, A.M., Emadi, A.: Discontinuous-conduction mode dc/dc converters feeding constant-power loads. IEEE Trans. Ind. Electron. 57(4), 1318–1329 (2009)

20. Alawieh, A., Ortega, R., Pillai, H., Astolfi, A., Berthelot, E.: Voltage regulation of a boost converter in discontinuous conduction mode: A simple robust adaptive feedback controller. IEEE Control Syst. Mag. 33(3), 55–65 (2013)
21. Khaligh, A., Rahimi, A.M., Emadi, A.: Negative impedance stabilizing pulse adjustment control technique for dc/dc converters operating in discontinuous conduction mode and driving constant power loads. IEEE Trans. Veh. Technol. 56(4), 2005–2016 (2007)
22. Xu, Q., Vafamand, N., Chen, L., Dragičević, T., Xie, L., Blaabjerg, F.: Review on advanced control technologies for bidirectional dc/dc converters in dc microgrids. IEEE J. Emerging Sel. Topics Power Electron. 9(2), 1205–1221 (2020)
23. He, W., Ortega, R.: Design and implementation of adaptive energy shaping control for dc–dc converters with constant power loads. IEEE Trans. Ind. Inf. 16(8), 5053–5064 (2019)
24. Ortega, R., Perez, J.A.L., Nicklasson, P.J., Sira Ramirez, H.J.: Passivity-Based Control of Euler-Lagrange Systems: Mechanical, Electrical and Electromechanical Applications. Springer Science & Business Media, Singapore (2013)
25. Ortega, R., Van Der Schaft, A., Maschke, B., Escobar, G.: Interconnection and damping assignment passivity-based control of port-controlled hamiltonian systems. Automatica 38(4), 585–596 (2002)
26. Sira Ramirez, H., Perez Moreno, R., Ortega, R., Garcia Esteban, M.: Passivity-based controllers for the stabilization of dc-to-dc power converters. Automatica 33(4), 499–513 (1997)
27. Sira Ramirez, H.J., Silva Ortigoza, R.: Control Design Techniques in Power Electronics devices. Springer Science & Business Media, Singapore (2006)
28. Shipra, K., Sharma, S.N., Maurya, R.: Passivity-based controllers for zvs quasi-resonant boost converter. IET Control Theory Appl. 14(20), 3461–3475 (2020)
29. Cimini, G., Ippoliti, G., Orlando, G., Pirro, M.: Sensorless power factor control for mixed conduction mode boost converter using passivity-based control. IET Power Electron. 7(12), 2988–2995 (2014)
30. Serra, F.M., Magaldi, G.L., Fernandez, L.M., Larregay, G.O., CH, D.A.: Ida-pbc controller of a dc-dc boost converter for continuous and discontinuous conduction mode. IEEE Lat. Am. Trans. 16(1), 52–58 (2018)
31. He, W., Li, S., Yang, J., Wang, Z.: Incremental passivity based control for dc-dc boost converters under time-varying disturbances via a generalized proportional integral observer. J. Power Electron. 18(1), 147–159 (2018)
32. Namazi, M.M., Nejad, S.M.S., Tabesh, A., Rashidi, A., Liserre, M.: Passivity-based control of switched reluctance-based wind system supplying constant power load. IEEE Trans. Ind. Electron. 65(12), 9550–9560 (2018)
33. Soloperto, R., Nahata, P., Tucci, M., Ferrari Trecate, G. A passivity-based approach to voltage stabilization in dc microgrids. In: 2018 Annual American Control Conference (ACC), pp. 5374–5379. IEEE, Piscataway (2018)
34. Pérez, M., Ortega, R., Espinoza, J.R.: Passivity-based pi control of switched power converters. IEEE Trans. Control Syst. Technol. 12(6), 881–890 (2004)
35. Hernandez Gomez, M., Ortega, R., Lamnabhi Lagarrigue, F., Escobar, G.: Adaptive pi stabilization of switched power converters. IEEE Trans. Control Syst. Technol. 18(3), 688–698 (2009)
36. Liu, J., Liu, Z., Su, H.: Passivity-based pi control for receiver side of dynamic wireless charging system in electric vehicles. IEEE Trans. Ind. Electron. 69(1), 783–794 (2021)
37. Bergna Diaz, G., Zonetti, D., Sanchez, S., Ortega, R., Tedeschi, E.: Pi passivity-based control and performance analysis of mmc multiterminal hvdc systems. IEEE J. Emerging Sel. Topics Power Electron. 7(4), 2453–2466 (2018)
38. Cisneros, R., Gao, R., Ortega, R., Husain, I.: A pi+ passivity-based control of a wind energy conversion system enabled with a solid-state transformer. Int. J. Control 94(9), 2453–2463 (2020)
39. Mojallizadeh, M.R., Badamchizadeh, M.A.: Adaptive passivity-based control of a photovoltaic/battery hybrid power source via algebraic parameter identification. IEEE J. Photovoltaics 6(2), 532–539 (2016)
40. He, W., Ortega, R., Machado, J.E., Li, S.: An adaptive passivity-based controller of a buck-boost converter with a constant power load. Asian J. Control 21(1), 581–595 (2019)
41. Soriano Rangel, C.A., He, W., Mancilla David, F., Ortega, R.: Voltage regulation in buck–boost converters feeding an unknown constant power load: An adaptive passivity-based control. IEEE Trans. Control Syst. Technol. 29(1), 395–402 (2020)
42. He, W., Soriano Rangel, C.A., Ortega, R., Astolfi, A., Mancilla David, F., Li, S.: Energy shaping control for buck–boost converters with unknown constant power load. Control Eng. Pract. 74, 33–43 (2018)
43. Montoya, O.D., Gil González, W., Serra, F.M., Magaldi, G. Pbc approach applied on a dc-dc step-down converter for providing service to cpls. In: 2019 IEEE 4th Colombian Conference on Automatic Control (CCAC), pp. 1–6. IEEE, Piscataway (2019)
44. Pang, S., Nahid Mobarakeh, B., Pierfederici, S., Phattanasak, M., Huangfu, Y., Luo, G., et al.: Interconnection and damping assignment passivity-based control applied to on-board dc–dc power converter system supplying constant power load. IEEE Trans. Ind. Appl. 55(6), 6476–6485 (2019)
45. Pang, S., Nahid Mobarakeh, B., Pierfederici, S., Huangfu, Y., Luo, G., Gao, F.: Towards stabilization of constant power loads using ida-pbc for cascaded lc filter dc/dc converters. IEEE J. Emerging Sel. Topics Power Electron. 9(2), 1302–1314 (2019)
46. Jeung, Y.C., Lee, D.C., Dragičević, T., Blaabjerg, F.: Design of passivity-based damping controller for suppressing power oscillations in dc microgrids. IEEE Trans. Power Electron. 36(4), 4016–4028 (2020)
47. Hassan, M.A., Su, C.L., Chen, F.Z., Lo, K.Y.: Adaptive passivity-based control of dc-dc boost power converter supplying constant power and constant voltage loads. IEEE Trans. Ind. Electron. (2021)
48. Kwasinski, A., Krein, P.T. Passivity-based control of buck converters with constant-power loads. In: 2007 IEEE Power Electronics Specialists Conference, pp. 259–265. IEEE, Piscataway (2007)
49. Kwasinski, A., Onwuchekwa, C.N.: Dynamic behavior and stabilization of dc microgrids with instantaneous constant-power loads. IEEE Trans. power Electron. 26(3), 822–834 (2010)
50. Hassan, M.A., Li, E.P., Li, X., Li, T., Duan, C., Chi, S.: Adaptive passivity-based control of dc–dc buck power converter with constant power load in dc microgrid systems. IEEE J. Emerging Sel. Topics Power Electron. 7(3), 2029–2040 (2018)
51. Astolfi, A., Karagiannis, D., Ortega, R.: Nonlinear and Adaptive Control with Applications. Springer Science & Business Media, Singapore (2007)
52. Zhang, M., Borja, P., Ortega, R., Liu, Z., Su, H.: Pid passivity-based control of port-hamiltonian systems. IEEE Trans. Autom. Control 63(4), 1032–1044 (2017)
53. Isidori, A., Sontag, E., Thoma, M.: Nonlinear Control Systems. vol. 3, Springer, Berlin/Heidelberg (1995)
54. Sepulchre, R., Jankovic, M., Kokotovic, P.V.: Constructive Nonlinear Control. Springer Science & Business Media, Singapore (2012)

How to cite this article: He, W., Namazi, M.M., Koofigar, H.R., Amirian, M.A., Blaabjerg, F. Stabilization of DC–DC buck converter with unknown constant power load via passivity-based control plus proportion-integration. IET Power Electron. 2021;14:2597–2609.
https://doi.org/10.1049/pel2.12205